CFD Letters 14, Issue 12 (2022) 111-125

CFD Letters

Journal homepage:
https://semarakilmu.com.my/journals/index.php/CFD_Letters/index
ISSN: 2180-1363

Flow of Casson Nanofluid Past a Permeable Surface: Effects of Brownian Motion, Thermophoretic Diffusion and Lorenz force

V. Seethamahalakshmi[1], P. Bindu[2], G. Venkata Ramana Reddy[2,*], Abayomi Samuel Oke[3]

[1] Department of Mathematics, PVP Siddartha Institute of Technology, Kanuru, Vijayawada, Andhra Pradesh 520007, India
[2] Department of Engineering Mathematics, Koneru Lakshmaiah Education Foundation, Vaddeswaram, Andhra Pradesh 522302, India
[3] Adekunle Ajasin University, P. M. B. 001, Akungba-Akoko, Ondo State, Nigeria

ARTICLE INFO

Article history:
Received 25 July 2022
Received in revised form 17 August 2022
Accepted 8 September 2022
Available online 31 December 2022

Keywords:
Casson nano liquid; MHD; Inclined porous surface; thermal Radiation

ABSTRACT

This study is aimed at testing the significance of Brownian movement and thermophoresis dispersion on MHD Casson nano liquid limit layer stream past a nonlinear slanted permeable extending surface, with the impact of convective limits and warm radiation with a synthetic response. Nonlinear ODEs are gotten from overseeing nonlinear PDEs by utilizing good comparability changes. The amounts related to building angles, for example, skin grating, Nusselt and Sherwood numbers alongside different effects of factors from the material on the speed and temperature, are outlined. Numerical consequences of the current investigation are acquired through the Runge-Kutta Fehlberg strategy alongside the shooting procedure and in a constraining sense are diminished to the distributed outcomes for a precision reason.

1. Introduction

Researchers, engineers and scientists have been paying attention to non-Newtonian fluids because of their numerous applications such as the production of food, annealing, etc. Also, there are several manufacturing processes in industries due to non-Newtonian fluids. They are biological fluids, lubricants, paints, polymeric suspensions etc. Several models such as the pseudo plastic model, Ellis model, power-law model, viscoelastic model etc. have been examined with different rheological equations and solved numerically in literature. Due to their complexity alongside nonlinearity, rheological equations of different types have been used by authors in literature to describe non-Newtonian fluids.

Casson fluid behaviour is different from all other types of non-Newtonian fluids. It is a shear-thinning fluid with an indefinite zero viscosity shear rate and vice versa. Examples of fluid that portrays this type of behaviour are orange juice, toothpaste, honey, tomato sauce, human blood and soup. Hayat *et al.,* [1] critically examined Casson fluid behaviour flowing on a stretchable surface. Ugwah-Oguejiofor *et al.,* [2] presented the influence of melting on the MHD Casson liquid flow past a stretchable permeable sheet. Kamran *et al.,* [3] elucidate Casson nanofluid MHD flow. They

* *Corresponding author.*
E-mail address: gvrr1976@kluniversity.in (G. Venkata Ramana Reddy)

https://doi.org/10.37934/cfdl.14.12.111125

obtained the solution of their flow equations numerically. Reddy and Krishna [4] pondered the Soret and Dufour effects on an MHD micropolar fluid flow over a linearly stretching sheet, through a non-Darcy porous medium. They numerically solved their model using the method for Runge-Kutta along with shooting technique. Shah *et al.,* [5] studied the model of Cattaneo-Christov for Casson ferrofluids past a stretchable sheet. The outcomes of their flow model were obtained using the homotopy analysis approach. Sodium alginate is another type of Casson liquid that many researchers have recently pondered on because of its applications in pharmaceuticals, textiles as well as cosmetics. Sodium alginate is highly viscous, it has solubility properties and is very safe. It is a type of Casson nano liquid. This type of fluid helps to enhance the fluid thermal properties. Khan *et al.,* [6] explored Sodium alginate MHD Casson nanofluid through a penetrable medium. In recent times, Alwawi *et al.,* [7] illustrated the movement of Sodium alginate Casson nano liquid past a solid sphere under the influence of magnetic force. Sandhya *et al.,* [8] presented the heat and mass transfer effects on MHD flow past an inclined porous plate in the presence of chemical reaction.

The study of nanofluids is seriously trending in recent years. It is mostly treated as a mixture made of a base fluid together with a nanoparticle. The nanofluid portrays a characteristic of a rise in the thermal conductivity of the basic liquid. The major thing that interests researchers that have studied the behaviour of nanofluids is because of its applications in engineering such as therapy, food processing, biological materials, photodynamics etc. The study conducted by Dolatabadi *et al.,* [9] introduced the concept of nanofluids. In another study by Buongiorno [10], nanoparticles alongside the convective transport of nanofluids were extensively discussed. After the study of Dolatabadi *et al.,* [9] and Buongiorno *et al.,* [11], many authors have analyzed the Buongiorno model with nanofluids. Ajam *et al.,* [12] elucidate MHD nanofluid flow on a stretchable and penetrable plate by employing Buongiorno's model. They obtained solutions to their equations using an analytical approach and they discovered that a large Biot number enhances the heat transport coefficient. Reddy *et al.,* [13] numerically observed the MHD slip flow of Carreau nanofluid by considering chemical reactions along with the Soret-Dufour mechanism. The model was solved using numerical techniques and inferred that a hike in thermophoresis lead to a spike in Nusselt number. Jaradat *et al.,* [14] discussed the two-mode coupled Burger's equation. Idowu and Falodun [15] recently discussed MHD flow of nanofluid of non-Newtonian base-fluid. The models were investigated numerically, and they came to a conclusion that the strength of the imposed magnetic field inhibits the velocity. Gangaiah *et al.,* [16] elucidated the impact of thermal radiation on the mixed convection MHD flow of Casson nanofluid. Rafique *et al.,* [17] elucidate Buongiorno model analysis together with Brownian alongside thermophoretic diffusion for Casson nano liquid. Lund *et al.,* [18] investigated MHD flow of micropolar nano liquid with buoyancy impact. The transformed ODE was solved numerically. They concluded that increasing Richardson number declines the micropolar nanofluid velocity.

Investigation of heat transport along a slanting porous surface has importance in the production of paper, drawing of glass, plastic film, wire drawing etc. Reddy *et al.,* [19] by considering the numerical solution of MHD, Soret, Dufour, and thermal radiation contributions on unsteady free convection motion of Casson liquid past a semi-infinite vertical porous plate. MHD free convective flow past a vertical porous plate in the presence of radiation and heat generation was studied by Mangathai *et al.,* [20]. Gurrampati *et al.,* [21] studied the similarity transformations of heat and mass transfer effects on steady MHD free convection dissipative fluid flow past an inclined porous surface with chemical reaction.

El-Dabe *et al.,* [22] explained heat along with mass transport of second-grade fluid flow. Heat transport of nanofluids is applicable in areas such as science and technology. Heat transport enhancements in the free convection flow of nanofluids have been studied by Aman *et al.,* [23].

Rashidi and Pour [24] discussed unsteady flow along with heat transfer because of a stretchable sheet. Motsa and Makukula [25] elucidate boundary layer flow heat alongside mass transport because of a stretchable surface. Singh and Agarwal [26] discussed the flow and heat transport of Maxwell liquid under the impact of variable thermo-physical parameters. Khidir and Sibanda [27] closely analysed MHD flow on the transfer of mass and heat on a rotating permeable disk. Idowu and Falodun [28] studied how Soret-Dufour's affect MHD flow and heat alongside the mass transfer of Walter's-B liquid. The recent study by the effects of Soret number and heat source on unsteady MHD Casson fluid flow past an inclined plate embedded on porous medium by Manjula and Sekhar [29].

Thermophoresis explains the migration of small particles towards degenerating thermal gradient by the thermophoretic force. The particles are driven right from a hot to a cold surface. An example of such a particle is dust. The consideration of thermophoresis together with Brownian motion is trending in recent research due to its relevance in science and industries. The impacts of thermophoresis on unsteady Oldroyd-B nano liquid flow were elucidated by Awad *et al.,* [30]. Mallikarjuna *et al.,* [30] examined thermophoresis along with transpiration's impact on non-Darcy convective flow. They applied a numerical method to solve the model and they discovered that velocity changes according to thermophoretic variations. Shehzad *et al.,* [31] investigated the impact of thermophoresis along with Joule heating on Jeffrey radiative fluid flow. Reddy *et al.,* [32] elucidate the radiation and chemical reaction effects on MHD flow along a moving vertical porous plate. Reddy *et al.,* [33] elucidate the combined thermophoresis along with Brownian motion effects on the unsteadiness of MHD nano liquid flow. Meanwhile, many authors have done their research work on MHD fluid flows along the thermal radiation effects on vertical and stretching surface [34-43]. Khan *et al.,* [44] presented the effect of MHD flow and heat transfer of double stratified micropolar fluid over a vertical permeable shrinking/stretching sheet with chemical reaction and heat source. Jamali *et al.,* [45] investigated the effect of different types of stenosis on generalized power law model of blood flow in a bifurcated artery. Hamrelaine *et al.,* [46] explored an analysis of MHD Jeffery Hamel flow with suction/injection by homotopy analysis method.

The present study explored areas that have not been considered by researchers in previously published works. Inspired by the above-aforementioned literature, we hereby present in this paper the Brownian, thermophoretic diffusion movement and Buongiorno model for MHD Casson nanoliquid. The velocity and concentration alongside temperature profiles are illustrated with the aid of diagrams. Tables are used to display the computational findings for quantities of engineering importance.

2. Problem Description

Consider an incompressible, 2D, Casson nano liquid flow past a nonlinear slanting porous stretchable sheet slanted at γ, where $u_w(x) = ax^m$ is the extending distance and $u_\infty(x) = 0$ is ambient distance, where x signifies coordinate taken towards the extended sheet, a is a constant. Chemical reaction is assumed during the flow. The magnetic field B_0 is imposed normal to the flow track. The thermophoresis and Brownian motion impact are presumed. The temperature T and nanoparticle fraction C take the values T_w and C_w right at the wall. The attributes of thermal radiation are examined with a convective heating analysis with temperature T_f and heat exchange factor h_f proportional to x^{-1}. However, the structures for nano liquid temperature and mass partitions T_∞ and C_∞ are obtained at free stream, as presented in Figure 1.

Following the formulations in the previous studies, the governing equations are [35-48]

$$\frac{\partial u}{\partial x} + \frac{\partial v}{\partial y} = 0, \tag{1}$$

$$\nu\left(1+\frac{1}{\beta}\right)\frac{\partial^2 u}{\partial y^2} + g[\beta_T(T-T_\infty)+\beta_C(C-C_\infty)]\cos\gamma - \frac{\sigma B_0^2(x)}{\rho}u - \frac{\upsilon}{K}u = u\frac{\partial u}{\partial x} + v\frac{\partial u}{\partial y}, \tag{2}$$

$$u\frac{\partial T}{\partial x} + v\frac{\partial T}{\partial y} - \tau\left[D_B\frac{\partial C}{\partial y}\frac{\partial T}{\partial y} + \frac{D_T}{T_\infty}\left(\frac{\partial T}{\partial y}\right)^2\right] = \frac{\kappa}{\rho c_p}\frac{\partial^2 T}{\partial y^2} - \frac{1}{(\rho c_p)_f}\frac{\partial q_r}{\partial y}, \tag{3}$$

$$u\frac{\partial C}{\partial x} + v\frac{\partial C}{\partial y} = D_B\frac{\partial^2 C}{\partial y^2} + \frac{D_T}{T_\infty}\frac{\partial^2 T}{\partial y^2} - K_r(C-C_\infty). \tag{4}$$

Roseland radiation flux is

$$q_r = \frac{-4\sigma^*}{3k^*}\frac{\partial T^4}{\partial y}, \quad \tau = \frac{(\rho c)_p}{(\rho c)_f}. \tag{5}$$

The difference in temperature between the temperatures T and the free stream temperature T_∞ are small, and by leaving terms of higher order, the Taylor's simplification about T_∞ is

$$T^4 = T_\infty^3(4T - 3T_\infty). \tag{6}$$

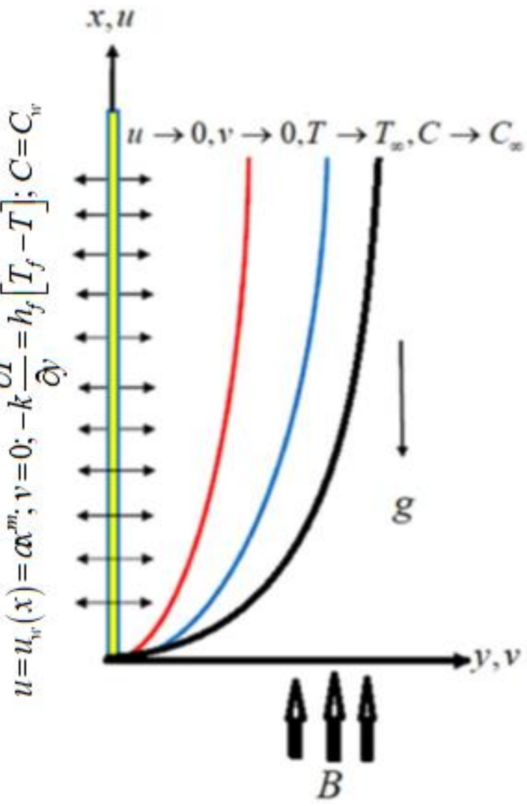

Fig. 1. Physical geometry

Putting Eq. (5) and Eq. (6) in Eq. (3) is simplified to

$$u\frac{\partial T}{\partial x} + v\frac{\partial T}{\partial y} = \left[\alpha + \frac{16\sigma^* T_\infty^3}{3k^*(\rho c)_f}\right]\frac{\partial^2 T}{\partial y^2} - +\tau\left[D_B\frac{\partial C}{\partial y}\frac{\partial T}{\partial y} + \frac{D_T}{T_\infty}\left(\frac{\partial T}{\partial y}\right)^2\right]. \tag{7}$$

The present analysis considered the boundary conditions (BCs) as:

$$u = u_w(x) = ax^m; v = 0; -k\frac{\partial T}{\partial y} = h_f\left[T_f - T\right]; C = C_w \text{ at } y = 0,$$
$$u \to u_\infty(x) = 0; v \to o; T \to T_\infty; C \to C_\infty \text{ at } y \to \infty. \quad (8)$$

The transformations variables are

$$\psi = \sqrt{\frac{2vax^{m+1}}{m+1}}f(\eta);\ \ \theta(\eta) = \frac{T-T_\infty}{T_w-T_\infty};\ \ \ \phi(\eta) = \frac{C-C_\infty}{C_w-C_\infty};\ \ \eta = y\sqrt{\frac{(m+1)ax^{m-1}}{2v}}. \quad (9)$$

Substituting Eq. (9) into Eq. (1) to Eq. (4), the following ordinary differential equations are obtained;

$$\left(1+\frac{1}{\beta}\right)f''' + ff'' - \frac{2m}{m+1}(f')^2 + \frac{2}{m+1}(\lambda\theta + \delta\phi)\cos\alpha - \frac{2}{m+1}\left(M + \frac{1}{K}\right)f' = 0, \quad (10)$$

$$\left(1+\frac{4R}{3}\right)\theta'' + \Pr f\theta' + \mathrm{PrNb}\theta'\phi' + \Pr Nb\,(\theta')^2 = 0, \quad (11)$$

$$\phi'' + (Nt/Nb)\theta'' + Lef\phi' - Kr\, Le\, \phi = 0, \quad (12)$$

The transformed boundary constraints are:

$$f(\eta) = 0;\ \ f'(\eta) = 1;\ \ \theta'(0) = -Bi\big(1-\theta(0)\big);\ \ \phi(\eta) = 1 \ \ \text{at } \eta = 0,$$
$$f'(\eta) \to 0;\ \ \theta(\eta) \to 0;\ \ \phi(\eta) \to 0 \quad \text{as } \eta \to \infty, \quad (13)$$

where

$$\lambda = \frac{Gr}{Re_x^2}; \delta = \frac{Gc}{Re_x^2}; M = \frac{\sigma B_0^2(x)x}{\rho u_w}; K = \frac{K_1 u_w}{vx}, \mathrm{N}_b = \frac{\tau D_B(C_w-C_\infty)}{\nu};$$
$$Nt = \frac{\tau D_T(T_w-T_\infty)}{\nu T_\infty}; Gr = \frac{g\beta_T(T_w-T_\infty)x^3}{\nu^2}; Gc = \frac{g\beta_C(C_w-C_\infty)x^3}{\nu^2}; \quad (14)$$
$$Le = \frac{\nu}{D_B}; Pr = \frac{\nu}{\alpha}, R_{e_x} = \frac{u_w x}{\nu}; R = \frac{4\sigma^* T_\infty^3}{k^* K}; Kr = \frac{2xK_r}{(m+1)u_w}, Bi = \frac{\eta}{k\sqrt{Re_x}}.$$

Here primes signify the differentiation wrt η. The skin friction, Sherwood as well as Nusselt numbers for the study are:

$$C_f = \frac{\tau_w}{u_w^2\rho f}, Nu = \frac{xq_w}{k(T_w-T_\infty)}; Sh = \frac{xq_m}{D_B(C_w-C_\infty)}; \quad (15)$$

where

$$q_w = -\left[k + \frac{4\sigma^* T_\infty^3}{3k^*}\right]\frac{\partial T}{\partial y};\ \ \ q_m = -D_B\frac{\partial C}{\partial y};\ \ \tau_w = \mu\left(1+\frac{1}{\beta}\right)\frac{\partial u}{\partial y} \quad \text{at } y = 0.$$

The dimensionless simplified Nusselt number $-\theta'(0)$, Sherwood number $-\phi'(0)$ and skin friction coefficient $C_f = \left(1+\frac{1}{\beta}\right)f''(0)$ are:

$$-\theta'(0) = \frac{Nu}{\left(1+\frac{4}{3}N\right)\sqrt{\left(\frac{m+1}{2}\right)Re_x}}; \quad -\phi'(0) = \frac{Sh}{\sqrt{\left(\frac{m+1}{2}\right)Re_x}}; \quad C_f = f''(0)\sqrt{\left(\frac{m+1}{2}\right)Re_x},$$

where $Re_x = \frac{u_w x}{\upsilon}$ is the local Reynolds number.

3. Outcomes and Discussion

The Runge-Kutta Fehlberg scheme with shooting technique is employed to investigate the results of the transformed ordinary differential equations of Eq. (10) to (12) with the BCs (13). The choice of this method is due to its wide stability region and the rate of convergence for boundary value problems have been established to be wide enough. The absolute error and the tolerance are set at 10^{-6}.

Flow parameters are varied and their significance on the flow are shown graphically and tabularly.

The main aim is based on the impact of Brownian movement along with thermophoresis on MHD Casson nano liquid limit layer over a nonlinear slanted permeable surface. The heat and mass transport problem were set up with thermophoresis, thermal radiation and Brownian motion. The flow model is solved numerically, and the physics of the problem is shown graphically. Also, we have computed values for the physical quantities of engineering importance and the results are shown in tables. Behaviours of pertinent flow parameters on local skin friction coefficient, Nusselt and Sherwood number are shown in Table 1. The results in Table 1 show that all the flow parameters enhance the transfer rate of mass and heat. This implies a great enhancement in the hydrodynamic and thermal boundary layer thickness. This demonstrates the use of this study in regulating the pace of cooling in heat transfer.

Figure 2 represents the magnetic and permeability terms' effects on the velocity plot. The magnetic parameter (M) is noticed to decline the velocity immediately after its value is increased. M has a significant effect on the fluid flow such that when it is applied transversely in the flow direction; it will produce the Lorentz force. In electromagnetism, Lorentz force is useful in engineering applications such as in plasma accelerators, MHD accelerators, hydrodynamic etc. Lorentz force is a phenomenon that slows the flow of an electrically conducting liquid. So, immediately the magnetic parameter increases more, it triggers the Lorentz force to decline the velocity as well as momentum boundary layer thickness. Also, a large permeability term (K) as shown in Figure 2 enhances the velocity profile. The presence of K allows the exchange of fluid particles among regions within the boundary layer. Now, increasing the value of K expands the pore size, hence providing space for more movement of fluid particles.

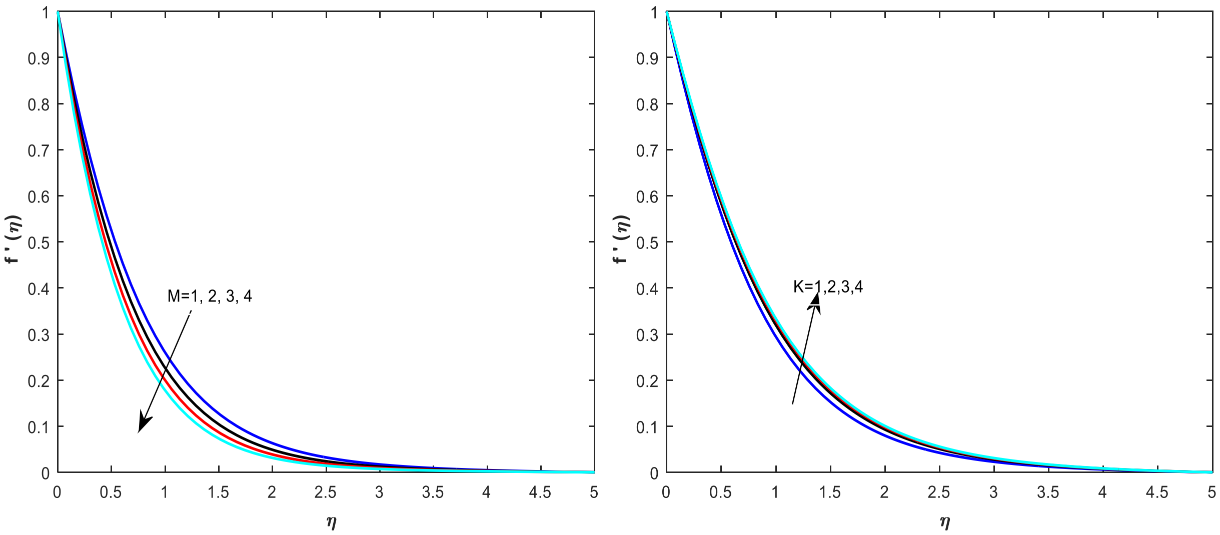

Fig. 2. Velocity profiles with magnetic and permeability parameters

Figure 3 shows the significance of the power index and the solutal buoyancy parameters on flow velocity. The power index parameter (m) enhances the velocity profile due to the existence of Brownian motion, thermophoresis along with Prandtl number. Hence, for a large value of m, the velocity profile increases. The solutal buoyancy parameter (δ) is observed to increase the velocity profile in Figure 3. Now, an increase in (δ) lead to large solutal buoyancy force and reduction in the viscosity which leads to increased velocity profile. Variation in the velocity profiles based on the impact of thermal buoyancy parameter (λ) and Casson parameter (β) is shown in Figure 4. The buoyancy force is noticed to increase the velocity profile as its value increases. Experimentally, an increase in λ lead to a reduction in the fluid viscosity which makes the fluid to thereby moves very fast. Therefore, increasing λ more leads to a drastic rise in the velocity profile (see Figure 4). The effect of β as shown in Figure 4 is observed to decrease velocity profiles. This can be traced to the fact β declines the yield stress in the Casson fluid. Hence, our experiment shows that β declines the yield stress meaning that plastic dynamic viscosity is improved which makes the momentum boundary layer to become very thick. The imposed magnetic field strength transversely to the flow direction is also a reason β degenerates the velocity profile. Figure 5 shows the impact of the inclination factor (α) on the velocity profile. An increase in α reduces the velocity profile. This is a reasonable result because the imposed magnetic field has a tendency of inhibiting fluid movement and declines the velocity profile due to an increase in α. In a moment $\alpha = 0$, it shows that the flow is subjected to the greatest gravitational force. The velocity profile drops the more at $\alpha = \frac{\pi}{2}$.

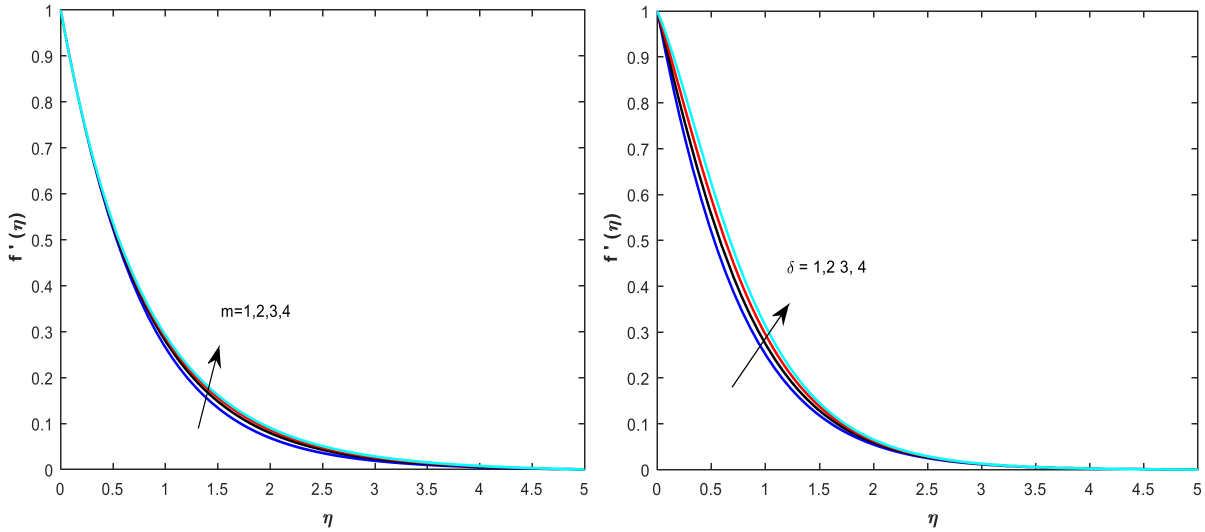

Fig. 3. Velocity profiles with power index and solutal buoyancy parameters

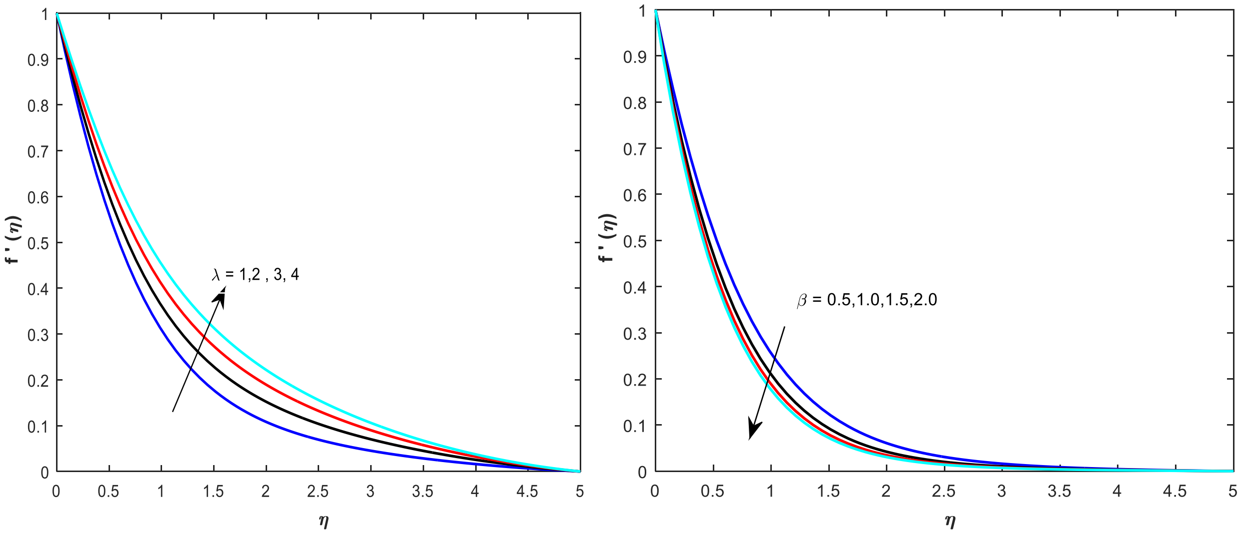

Fig. 4. Velocity profile with thermal buoyancy parameter and Casson parameter

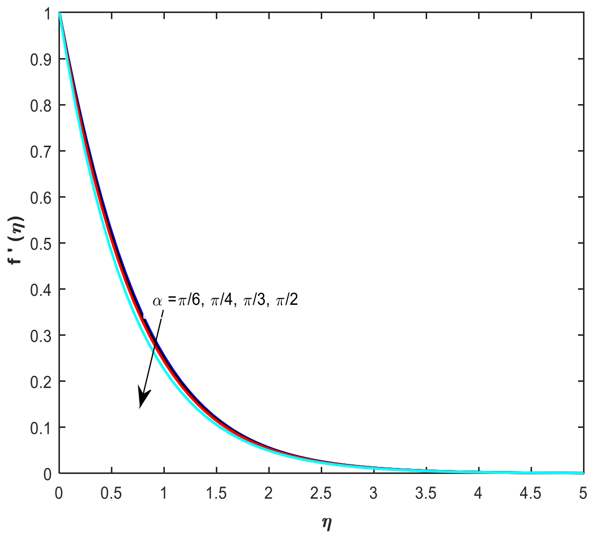

Fig. 5. Velocity profile with inclination factor

Figure 6 depicts the effect of the solutal buoyancy force parameter (λ) and Prandtl number (Pr) on the temperature profile. Raising α is observed to decrease the temperature profile. The solutal buoyancy parameter acts like a pull which slows down the motion of an electrically conducting fluid because of the presence of M and also, an increase in Pr is observed to reduce temperature profiles. Experimentally, the thermal conductivity of the fluid degenerates with increasing Pr. Hence, this leads to degeneration in the thermal boundary layer thickness. Figure 7 portrays the effects of radiation parameter (R) and Biot number (Bi) on the temperature profile. Thermal radiation shows a great impact on the heat transfer rate of the flow. The thermal radiation parameter helps to boost the rate of heat transport. Hence, raising R enhances the thermal condition of the fluid by enhancing the temperature profile along with the thickness of the thermal boundary layer. It is also observed that an increase in Biot number boosts the temperature (see Figure 7). Hence, as Bi increases, the heat transport coefficient also increases. However, this increases in heat transport coefficient increased fluid temperature.

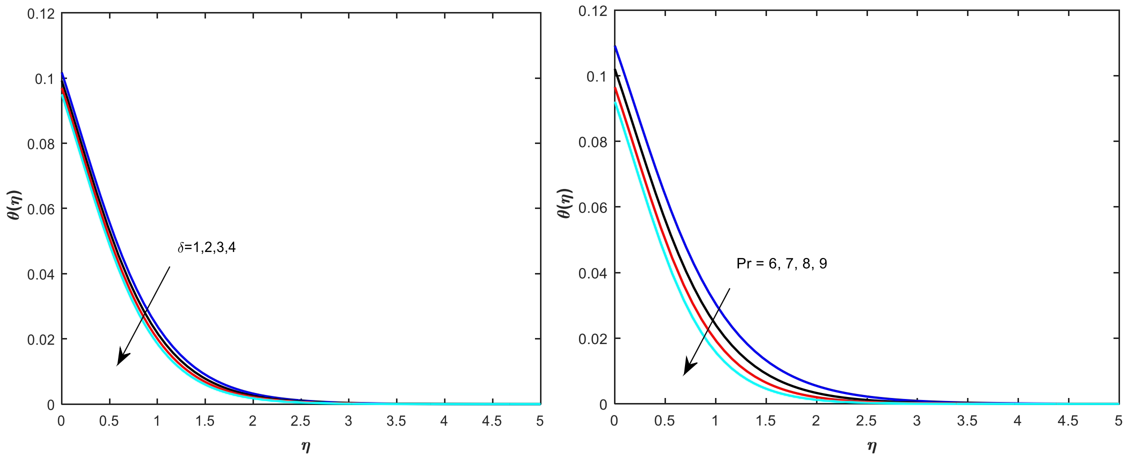

Fig. 6. Concentration profiles with solutal buoyancy parameter and Prandtl number

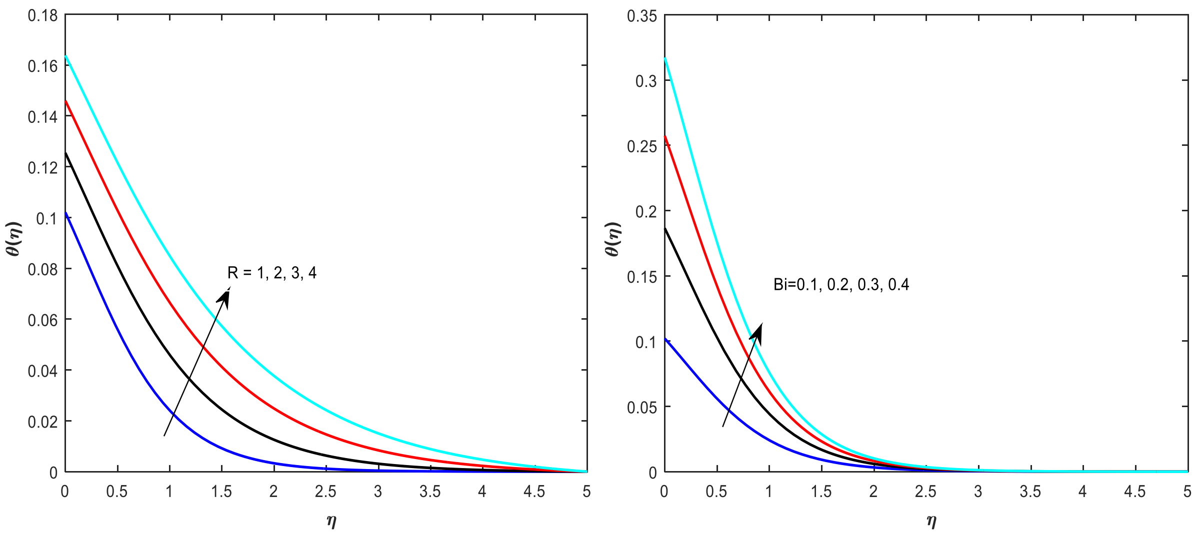

Fig. 7. Temperature profile with thermal radiation parameter and Biot number

Figure 8 portrays the impact of Brownian motion (Nb) and thermophoresis (Nt) on the temperature profile. Increasing the value of both Nb and Nt is observed to boost the temperature profile. This in return enhances the rate of heat transport. This means that the Brownian motion mechanism could be useful in distributing the nano-particles in the flow regime. Also, a small value of Nb and Nt could be useful in cooling the flow regime. Figure 9 shows the impact of the inclination factor (α) on the temperature profile. Increasing α is noticed to enhance the fluid temperature profile and the entire boundary layer thickness. Figure 10 depicts the impact of Nb and Nt on the concentration profile. An increase in the value of Nb is observed to degenerate the fluid concentration profile while the increase in the value of Nt enhances the fluid concentration profile. This shows that the thermophoresis parameter (Nt) helps the nanoparticle diffusion in the boundary layer. Also, the concentration boundary layer thickness becomes very low because of an increase in the Brownian motion parameter (Nb). Figure 11 shows the effect of the chemical reaction parameter (Kr) and Lewis number (Le) on the concentration profile. Lewis number is a dimensionless number which portrays the contribution of the rate of thermal diffusion to the rate of species diffusion. It is derived from the ratio of the Schmidt number to the Prandtl number. Therefore, when Le=1, heat alongside species diffuses at the same rate but when$Le > 1$, heat diffuses faster than species. Also, an increase in the value of Kr is seen to be destructive to the concentration profile as increasing Kr degenerates the concentration profile. Figure 12 represents the effect of the inclination factor (α) on the concentration profile. A gradual increase in α is observed to give a slight increase to the concentration profile.

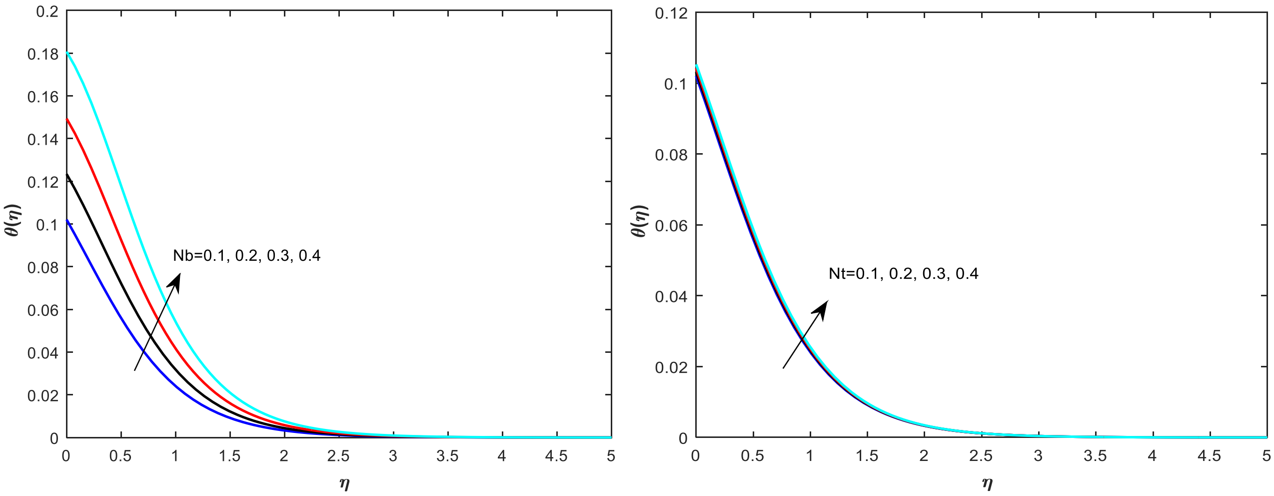

Fig. 8. Temperature profile with Brownian motion and thermophoresis parameter

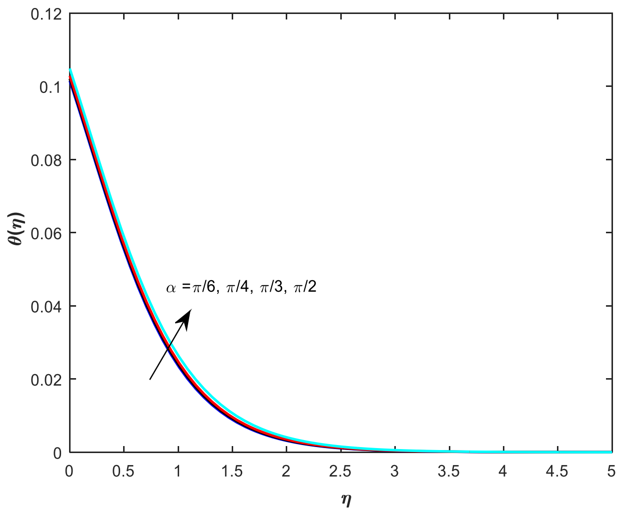

Fig. 9. Temperature profile with inclination factor

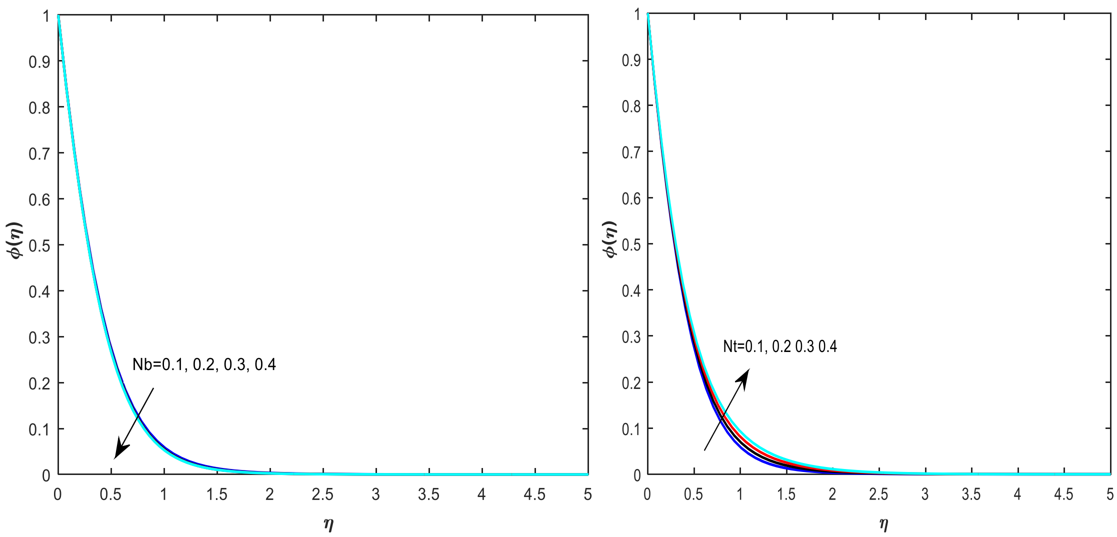

Fig. 10. Concentration profile with Brownian motion and thermophoresis parameter

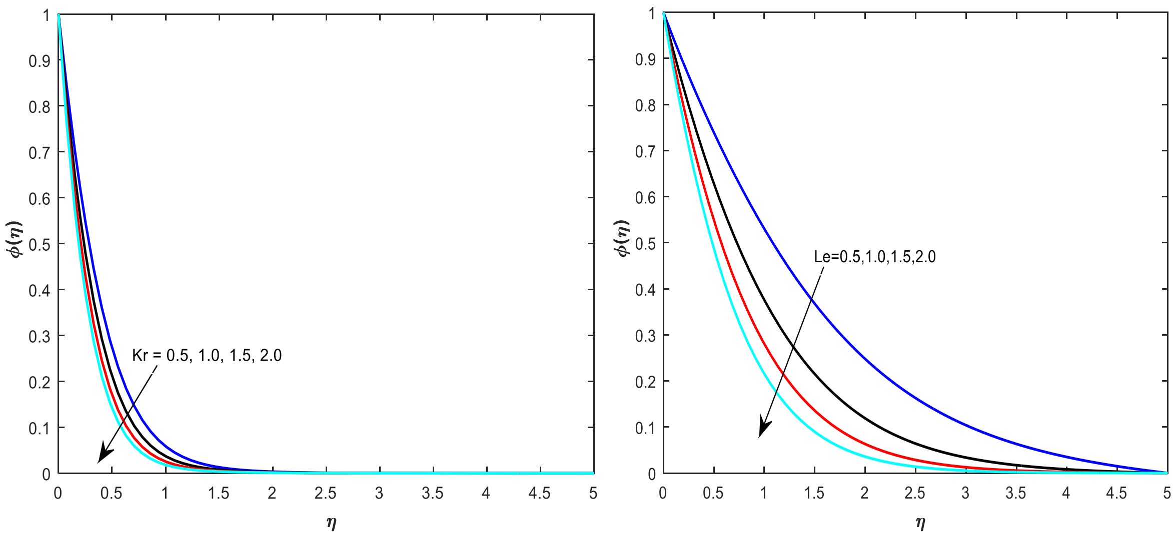

Fig. 11. Concentration profile with chemical reaction parameter and Lewis number

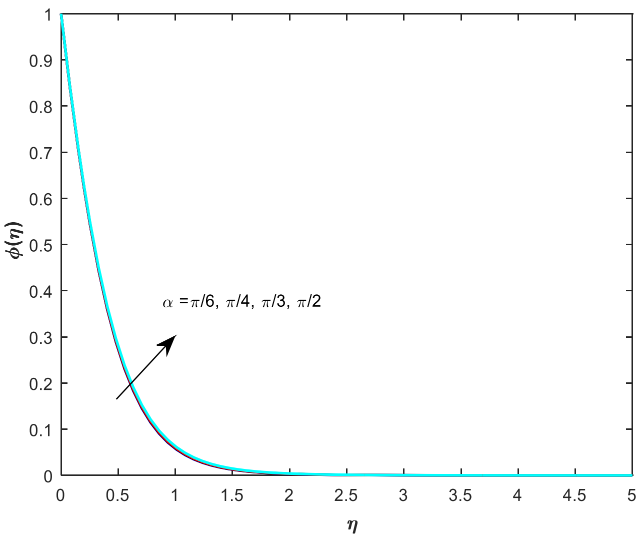

Fig. 12. Concentration profile with inclination factor

Table 1
Computational values of different flow parameters on local skin friction, Nusselt and Sherwood number

M	K	m	λ	δ	β	Pr	R	Nb	Nt	Kr	Le	α	Bi	Cf	Nu	Sh
1														1.233354	0.072799	2.131724
2	0.5													1.383640	0.073107	2.144011
3														1.521480	0.073466	2.157612
4		0.5												1.649481	0.073892	2.172872
	1													0.927143	0.074411	2.190304
	2													0.943393	0.074718	2.200075
	3		0.9											0.975295	0.074829	2.203521
	4													1.066662	0.074886	2.205283
		1		0.1										1.248577	0.074017	2.174142
		2												1.262181	0.074168	2.175710
		3			0.5									1.268252	0.074254	2.176629
		4				0.71								1.271624	0.074311	2.177230
			1											0.553403	0.089823	2.156779
			2				1							0.770516	0.090079	2.174759
			3											0.992048	0.090299	2.191762
			4											1.218581	0.090493	2.207915
				1				0.1						0.729060	0.074638	2.190333
				2										0.841156	0.075284	2.205774
				3					0.1					0.959843	0.075825	2.219696
				4										1.086907	0.076291	2.232448
										0.5	5			1.210731	0.072833	2.133445
					1									1.431945	0.073013	2.140694
					1.5									1.552122	0.073314	2.152397
					2							$\frac{\pi}{4}$		1.628086	0.073928	2.174682
					0.5	6								1.241202	0.089083	2.153118
						7								1.241536	0.089796	2.153932
						8								1.241788	0.090348	2.154921
						9							0.1	1.241985	0.090789	2.156133
						7	1							1.238474	0.083620	2.154921
							2							1.239388	0.085402	2.158643
							3							1.240417	0.087457	2.161399
							4							1.241536	0.089796	2.163519
								0.1						1.241109	0.081929	2.154921
	0.5							0.2						1.241536	0.085064	2.171138
								0.3						1.242169	0.087661	2.177223
		0.5						0.4						1.242634	0.089796	2.180837
								0.1						1.228234	0.089470	2.096771
			0.9						0.2					1.232675	0.089582	2.115110
									0.3					1.237109	0.089690	2.134505
				0.1					0.4					1.241536	0.089796	2.154921
									0.1					1.241536	0.089434	2.154921
					0.5					1				1.264279	0.089517	2.678377
										1.5				1.280017	0.089630	3.115223
						7				2				1.291853	0.089796	3.497552
											0.5			1.033845	0.090424	0.582769
							1				1			1.095579	0.090632	0.874960
											1.5			1.133928	0.090917	1.104605
								0.1			2			1.161051	0.091341	1.299896
												$\frac{\pi}{6}$		1.194393	0.089515	2.137252
												$\frac{\pi}{4}$		1.241536	0.089718	2.149859
										0.5		$\frac{\pi}{3}$		1.303363	0.089796	2.154921
											5	$\frac{\pi}{2}$		1.454565	0.089853	2.158746
												$\frac{\pi}{4}$	0.1	1.225173	0.089796	2.114918
													0.2	1.229707	0.162697	2.125481
													0.3	1.235082	0.222809	2.138521
													0.4	1.241536	0.273073	2.154921

4. Conclusion

The Runge-Kutta Fehlberg together with the shooting procedure is utilized on the transformed differential equation of Eq. (10) to (12) subject to (13) which describe the Brownian, thermophoretic diffusion and Buongiorno model for MHD Casson nanoliquid flow with convective boundary constraints. The method used in this study agreed very close to previously published works. The key findings in the present study are:

I. A large value of M is noticed to degenerate the velocity profile;
II. The velocity profile degenerates with a large value of β;
III. The Biot number (Bi) is noticed to increase the heat transport coefficient;
IV. A large value of Nb and Nt is observed to boost the temperature profile; and
V. All pertinent flow parameters are noticed to enhance the rate of heat and mass transport by increasing the local skin friction coefficient, Nusselt and Sherwood number.

References

[1] Hayat, T., S. A. Shehzad, A. Alsaedi, and M. S. Alhothuali. "Mixed convection stagnation point flow of Casson fluid with convective boundary conditions." *Chinese Physics Letters* 29, no. 11 (2012): 114704. https://doi.org/10.1088/0256-307X/29/11/114704

[2] Ugwah-Oguejiofor, Chinenye Jane, Charles Ogbonna Okoli, Michael Oguejiofor Ugwah, Millicent Ladi Umaru, Chiedozie Smart Ogbulie, Halilu Emmanuel Mshelia, Mohammed Umar, and Anoka Ayembe Njan. "Acute and sub-acute toxicity of aqueous extract of aerial parts of Caralluma dalzielii NE Brown in mice and rats." *Heliyon* 5, no. 1 (2019): e01179. https://doi.org/10.1016/j.heliyon.2019.e01179

[3] Kamran, A., S. Hussain, M. Sagheer, and N. Akmal. "A numerical study of magnetohydrodynamics flow in Casson nanofluid combined with Joule heating and slip boundary conditions." *Results in Physics* 7 (2017): 3037-3048. https://doi.org/10.1016/j.rinp.2017.08.004

[4] Reddy, G. V. R., and Y. Hari Krishna. "Soret and dufour effects on MHD micropolar fluid flow over a linearly stretching sheet, through a non-darcy porous medium." *International Journal of Applied Mechanics and Engineering* 23, no. 2 (2018). https://doi.org/10.2478/ijame-2018-0028

[5] Shah, Zahir, Abdullah Dawar, I. Khan, Saeed Islam, Dennis Ling Chaun Ching, and Aurang Zeb Khan. "Cattaneo-Christov model for electrical magnetite micropoler Casson ferrofluid over a stretching/shrinking sheet using effective thermal conductivity model." *Case Studies in Thermal Engineering* 13 (2019): 100352. https://doi.org/10.1016/j.csite.2018.11.003

[6] Khan, Arshad, Dolat Khan, Ilyas Khan, Farhad Ali, and Muhammad Imran. "MHD flow of sodium alginate-based Casson type nanofluid passing through a porous medium with Newtonian heating." *Scientific Reports* 8, no. 1 (2018): 1-12. https://doi.org/10.1038/s41598-018-26994-1

[7] Alwawi, Firas A., Hamzeh T. Alkasasbeh, A. M. Rashad, and Ruwaidiah Idris. "MHD natural convection of Sodium Alginate Casson nanofluid over a solid sphere." *Results in Physics* 16 (2020): 102818. https://doi.org/10.1016/j.rinp.2019.102818

[8] Sandhya, A., G. V. Ramana Reddy, and V. S. R. G. Deekshitulu. "Heat and mass transfer effects on MHD flow past an inclined porous plate in the presence of chemical reaction." *International Journal of Applied Mechanics and Engineering* 25, no. 3 (2020). https://doi.org/10.2478/ijame-2020-0036

[9] Dolatabadi, Nader, Ramin Rahmani, Homer Rahnejat, and Colin P. Garner. "Thermal conductivity and molecular heat transport of nanofluids." *RSC Advances* 9, no. 5 (2019): 2516-2524. https://doi.org/10.1039/C8RA08987F

[10] Buongiorno, Jacopo. "Convective transport in nanofluids." *Journal of Heat Transfer* 128, no. 3 (2006): 240-250. https://doi.org/10.1115/1.2150834

[11] Buongiorno, Jacopo, Lin-Wen Hu, Sung Joong Kim, Ryan Hannink, B. A. O. Truong, and Eric Forrest. "Nanofluids for enhanced economics and safety of nuclear reactors: an evaluation of the potential features, issues, and research gaps." *Nuclear Technology* 162, no. 1 (2008): 80-91. https://doi.org/10.13182/NT08-A3934

[12] Ajam, Hossein, Seyed Sajad Jafari, and Navid Freidoonimehr. "Analytical approximation of MHD nano-fluid flow induced by a stretching permeable surface using Buongiorno's model." *Ain Shams Engineering Journal* 9, no. 4 (2018): 525-536. https://doi.org/10.1016/j.asej.2016.03.006

[13] Reddy, Seethi Reddy Reddisekhar, Polu Bala Anki Reddy, and Ali J. Chamkha. "Influence of Soret and Dufour effects on unsteady 3D MHD slip flow of Carreau nanofluid over a slendering stretchable sheet with chemical reaction." *Nonlinear Analysis: Modelling and Control* 24, no. 6 (2019): 853-869. https://doi.org/10.15388/NA.2019.6.1

[14] Jaradat, H. M., Muhammed Syam, Marwan Alquran, Safwan Al Shara, and Khedr M. Abohassn. "A new two-mode coupled Burgers equation: Conditions for multiple kink solution and singular kink solution to exist." *Ain Shams Engineering Journal* 9, no. 4 (2018): 3239-3244. https://doi.org/10.1016/j.asej.2017.12.005

[15] Idowu, A. S., and B. O. Falodun. "Effects of thermophoresis, Soret-Dufour on heat and mass transfer flow of magnetohydrodynamics non-Newtonian nanofluid over an inclined plate." *Arab Journal of Basic and Applied Sciences* 27, no. 1 (2020): 149-165. https://doi.org/10.1080/25765299.2020.1746017

[16] Gangaiah, T., N. Saidulu, and A. Venkata Lakshmi. "The Influence of Thermal Radiation on Mixed Convection MHD Flow of a Casson Nanofluid over an Exponentially Stretching Sheet." *International Journal of Nanoscience and Nanotechnology* 15, no. 2 (2019): 83-98.

[17] Rafique, Khuram, Muhammad Imran Anwar, Masnita Misiran, Ilyas Khan, Sayer O. Alharbi, Phatiphat Thounthong, and Kottakkaran Sooppy Nisar. "Keller-box analysis of Buongiorno model with Brownian and thermophoretic diffusion for Casson nanofluid over an inclined surface." *Symmetry* 11, no. 11 (2019): 1370. https://doi.org/10.3390/sym11111370

[18] Lund, Liaquat Ali, Zurni Omar, and Ilyas Khan. "Mathematical analysis of magnetohydrodynamic (MHD) flow of micropolar nanofluid under buoyancy effects past a vertical shrinking surface: Dual solutions." *Heliyon* 5, no. 9 (2019): e02432. https://doi.org/10.1016/j.heliyon.2019.e02432

[19] Reddy, K. Veera, G. Venkata Ramana Reddy, A. Sandhya, and Y. Hari Krishna. "Numerical solution of MHD, Soret, Dufour, and thermal radiation contributions on unsteady free convection motion of Casson liquid past a semi-infinite vertical porous plate." *Heat Transfer* 51, no. 3 (2022): 2837-2858. https://doi.org/10.1002/htj.22452

[20] Mangathai, P., G. V. Ramana Reddy, and B. Rami Reddy. "MHD free convective flow past a vertical porous plate in the presence of radiation and heat generation." *International Journal of Chemical Sciences* 14, no. 3 (2016): 1577-1597.

[21] Gurrampati, Venkata Ramana Reddy, S. Mohammed Ibrahim, and V. S. Bhagavan. "Similarity transformations of heat and mass transfer effects on steady MHD free convection dissipative fluid flow past an inclined porous surface with chemical reaction." *Journal of Naval Architecture and Marine Engineering* 11, no. 2 (2014): 157-166. https://doi.org/10.3329/jname.v11i2.18313

[22] El-Dabe, Nabil TM, A. Refaie Ali, A. A. El-shekhipy, and G. A. Shalaby. "Non-linear heat and mass transfer of second grade fluid flow with Hall currents and thermophoresis Effects." *Applied Mathematics & Information Sciences* 11, no. 1 (2017): 267-280. https://doi.org/10.18576/amis/110133

[23] Aman, Sidra, Ilyas Khan, Zulkhibri Ismail, Mohd Zuki Salleh, and Qasem M. Al-Mdallal. "Heat transfer enhancement in free convection flow of CNTs Maxwell nanofluids with four different types of molecular liquids." *Scientific Reports* 7, no. 1 (2017): 1-13. https://doi.org/10.1038/s41598-017-01358-3

[24] Rashidi, M. M., and S. A. Mohimanian Pour. "Analytic approximate solutions for unsteady boundary-layer flow and heat transfer due to a stretching sheet by homotopy analysis method." *Nonlinear Analysis: Modelling and Control* 15, no. 1 (2010): 83-95. https://doi.org/10.15388/NA.2010.15.1.14366

[25] Motsa, Sandile S., and Zodwa G. Makukula. "On a Bivariate Spectral Homotopy Analysis Method for Unsteady Mixed Convection Boundary Layer Flow, Heat, and Mass Transfer due to a Stretching Surface in a Rotating Fluid." *Journal of Applied Mathematics* 2017 (2017). https://doi.org/10.1155/2017/5962073

[26] Singh, V., and Sh Agarwal. "Flow and heat transfer of Maxwell fluid with variable viscosity and thermal conductivity over an exponentially stretching sheet." *American Journal of Fluid Dynamics* 3, no. 4 (2013): 87-95.

[27] Khidir, A. A., and P. Sibanda. "On spectral-homotopy analysis solutions of steady magnetohydrodynamic (MHD) flow and heat transfer from a rotating disk in a porous medium." *Scientific Research and Essays* 7, no. 31 (2012): 2770-2780.

[28] Idowu, A. S., and B. O. Falodun. "Soret-Dufour effects on MHD heat and mass transfer of Walter'sB viscoelastic fluid over a semi-infinite vertical plate: spectral relaxation analysis." *Journal of Taibah University for Science* 13, no. 1 (2019): 49-62. https://doi.org/10.1080/16583655.2018.1523527

[29] Manjula, V., and K. V. Chandra Sekhar. "Effect of Soret number and heat source on unsteady MHD Casson fluid flow past an inclined plate embedded in porous medium." *ARPN Journal of Engineering and Applied Sciences* 14, no. 11 (2019): 2069-2079.

[30] Mallikarjuna, B., A. M. Rashad, Ahmed Kadhim Hussein, and S. Hariprasad Raju. "Transpiration and thermophoresis effects on non-Darcy convective flow past a rotating cone with thermal radiation." *Arabian Journal for Science and Engineering* 41, no. 11 (2016): 4691-4700. https://doi.org/10.1007/s13369-016-2252-x

[31] Shehzad, S. A., A. Alsaedi, and T. Hayat. "Influence of thermophoresis and Joule heating on the radiative flow of Jeffrey fluid with mixed convection." *Brazilian Journal of Chemical Engineering* 30 (2013): 897-908. https://doi.org/10.1590/S0104-66322013000400021

[32] Reddy, G. V. Ramana, N. Bhaskar Reddy, and R. S. R. Gorla. "Radiation and chemical reaction effects on MHD flow along a moving vertical porous plate." *International Journal of Applied Mechanics and Engineering* 21, no. 1 (2016): 157-168. https://doi.org/10.1515/ijame-2016-0010

[33] Reddy, J. V. Ramana, V. Sugunamma, and N. Sandeep. "Thermophoresis and Brownian motion effects on unsteady MHD nanofluid flow over a slendering stretching surface with slip effects." *Alexandria Engineering Journal* 57, no. 4 (2018): 2465-2473. https://doi.org/10.1016/j.aej.2017.02.014

[34] Kigio, John Kinyanjui, Mutuku Winifred Nduku, and Oke Abayomi Samuel. "Analysis of volume fraction and convective heat transfer on MHD Casson nanofluid over a vertical plate." *Fluid Mechanics* 7, no. 1 (2021): 1-8. https://doi.org/10.11648/j.fm.20210701.11

[35] Reddy, Karnati Veera, and Gurrampati Venkata Ramana Reddy. "Outlining the Impact of Melting on Mhd Casson Fluid Flow Past a Stretching Sheet in a Porous Medium with Radiation." *Biointerface Research in Applied Chemistry* 13, no. 1 (2022): 1-14. https://doi.org/10.33263/BRIAC131.042

[36] Rani, K. Sandhya, and G. Venkata Ramana Reddy. "Cattaneo-Christov Heat and Mass Transfer Flux Across Electro-Hydrodynamics Blood-Based Hybrid NanoFluid Subject to Lorentz Force." *CFD Letters* 14, no. 7 (2022): 124-134. https://doi.org/10.37934/cfdl.14.7.124134

[37] Gurrampati, Venkata Ramana Reddy, and Kolli Vijaya. "The Buongiorno model with Brownian and thermophoretic diffusion for MHD casson nanofluid over an inclined porous surface." *Journal of Naval Architecture and Marine Engineering* 19, no. 1 (2022): 31-45.

[38] Gladys, T., and G. V. Ramana Reddy. "Contributions of variable viscosity and thermal conductivity on the dynamics of non-Newtonian nanofluids flow past an accelerating vertical plate." *Partial Differential Equations in Applied Mathematics* 5 (2022): 100264. https://doi.org/10.1016/j.padiff.2022.100264

[39] Reddy, K. Veera, G. Venkata Ramana Reddy, A. Sandhya, and Y. Hari Krishna. "Numerical solution of MHD, Soret, Dufour, and thermal radiation contributions on unsteady free convection motion of Casson liquid past a semi-infinite vertical porous plate." *Heat Transfer* 51, no. 3 (2022): 2837-2858. https://doi.org/10.1002/htj.22452

[40] Reddy, G. Venkata Ramana, K. V. Chandra Sekhar, and Bidemi Olumide Falodun. "Multiple Slip Effects on Unsteady MHD Casson Nanofluid Flow over a Porous Stretching Sheet." *Journal of Applied Nonlinear Dynamics* 11, no. 3 (2022): 651-666. https://doi.org/10.5890/jand.2022.09.009

[41] Kumar, K. Ganesh, M. Gnaneswara Reddy, M. V. V. N. L. Sudharani, S. A. Shehzad, and Ali J. Chamkha. "Cattaneo-Christov heat diffusion phenomenon in Reiner-Philippoff fluid through a transverse magnetic field." *Physica A: Statistical Mechanics and its Applications* 541 (2020): 123330. https://doi.org/10.1016/j.physa.2019.123330

[42] Magyari, Eugen, and Ali J. Chamkha. "Combined effect of heat generation or absorption and first-order chemical reaction on micropolar fluid flows over a uniformly stretched permeable surface: the full analytical solution." *International Journal of Thermal Sciences* 49, no. 9 (2010): 1821-1828. https://doi.org/10.1016/j.ijthermalsci.2010.04.007

[43] Takhar, Harmindar S., Ali J. Chamkha, and Girishwar Nath. "MHD flow over a moving plate in a rotating fluid with magnetic field, Hall currents and free stream velocity." *International Journal of Engineering Science* 40, no. 13 (2002): 1511-1527. https://doi.org/10.1016/S0020-7225(02)00016-2

[44] Khan, Ansab Azam, Khairy Zaimi, Suliadi Firdaus Sufahani, and Mohammad Ferdows. "MHD flow and heat transfer of double stratified micropolar fluid over a vertical permeable shrinking/stretching sheet with chemical reaction and heat source." *Journal of Advanced Research in Applied Sciences and Engineering Technology* 21, no. 1 (2020): 1-14. https://doi.org/10.37934/araset.21.1.114

[45] Jamali, Muhammad Sabaruddin Ahmad, Zuhaila Ismail, and Norsarahaida Saidina Amin. "Effect of Different Types of Stenosis on Generalized Power Law Model of Blood Flow in a Bifurcated Artery." *Journal of Advanced Research in Fluid Mechanics and Thermal Sciences* 87, no. 3 (2021): 172-183. https://doi.org/10.37934/arfmts.87.3.172183

[46] Hamrelaine, Salim, Fateh Mebarek-Oudina, and Mohamed Rafik Sari. "Analysis of MHD Jeffery Hamel flow with suction/injection by homotopy analysis method." *Journal of Advanced Research in Fluid Mechanics and Thermal Sciences* 58, no. 2 (2019): 173-186.

[47] Shafique, Ahmad, Muhammad Ramzan, Zaib Un Nisa, Mudassar Nazar, and Hafeez Ahmad. "Unsteady Magnetohydrodynamic Flow of Second Grade Nanofluid (Ag-Cu) With CPC Fractional Derivative: nanofluid." *Journal of Advanced Research in Fluid Mechanics and Thermal Sciences* 97, no. 2 (2022): 103-114. https://doi.org/10.37934/arfmts.97.2.103114

[48] Mahat, Rahimah, Muhammad Saqib, Imran Ulah, Sharidan Shafie, and Sharena Mohamad Isa. "MHD Mixed Convection of Viscoelastic Nanofluid Flow due to Constant Heat Flux." *Journal of Advanced Research in Numerical Heat Transfer* 9, no. 1 (2022): 19-25.